The John A. Blume Earthquake Engineering Center

Department of Civil Engineering
Stanford University

ANNUAL REPORT

to

United States Department of Interior
Geological Survey
Office of Earthquake Studies
Menlo Park, California 94025

Contract No. 14-08-0001-17766
June 1980

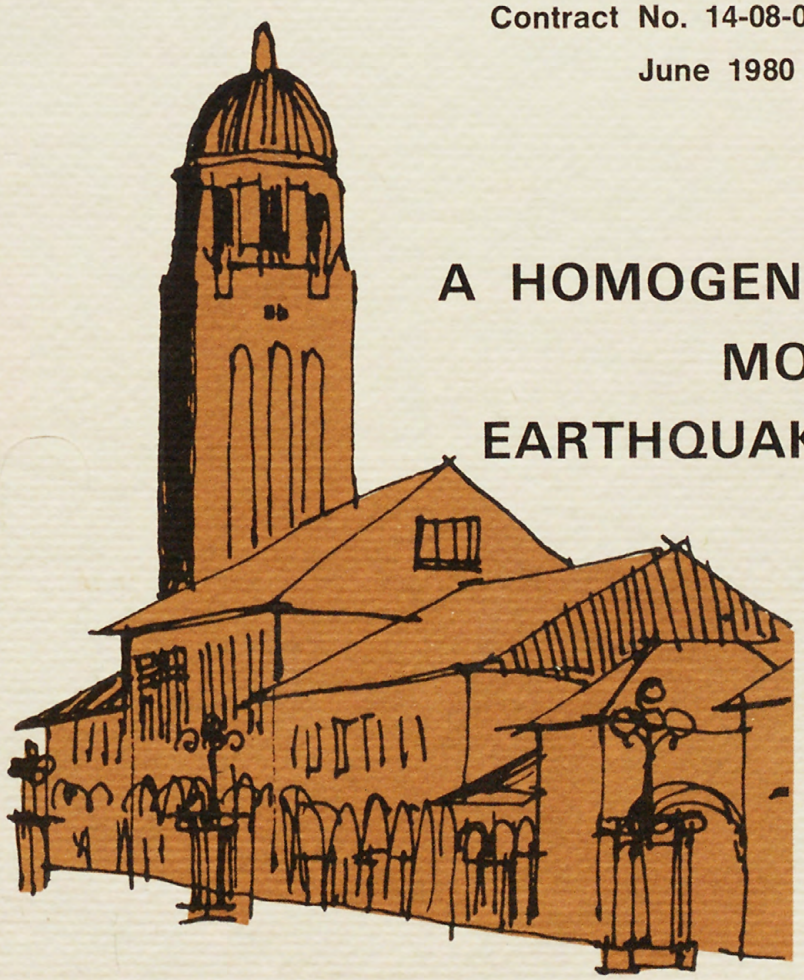

A HOMOGENEOUS STOCHASTIC MODEL FOR EARTHQUAKE OCCURRENCES

by

Anne S. Kiremidjian
Thalia Anagnos

The John A. Blume Earthquake Engineering Center was established to promote research and education in earthquake engineering. Through its activities our understanding of earthquakes and their effects on mankind's facilities and structures is improving. The Center conducts research, provides instruction, publishes reports and articles, conducts seminars and conferences, and provides financial support for students. The Center is named for Dr. John A. Blume, a well-known consulting engineer and Stanford alumnus.

Address

The John A. Blume Earthquake Engineering Center
Department of Civil Engineering
Stanford University
Stanford, California 94305

ANNUAL REPORT

to

United States Department of Interior
Geological Survey
Office of Earthquake Studies
Menlo Park, California 94025

Contract #14-08-0001-17766
June 1980

A HOMOGENEOUS STOCHASTIC MODEL FOR EARTHQUAKE OCCURRENCES

Anne S. Kiremidjian
Thalia Anagnos

Department of Civil Engineering
Stanford University
Stanford, California 94305

TABLE OF CONTENTS

LIST OF FIGURES

LIST OF TABLES

ACKNOWLEDGMENT

The continuous help of Professor Haresh C. Shah of the Department of Civil Engineering, is gratefully acknowledged.

We are also grateful to Tim Hall for valuable discussions on the activity of the San Andreas fault. Our thanks to Ram Kulkarni of Woodward-Clyde Consultants in San Francisco for providing the data on the circum-Pacific belt.

ERRATA

	PRESENTLY	CHANGE TO
p.8	$\{\pi^1(s_i, t_0 + \Delta t)\} = \underset{\sim}{P}(S_i, t_0)\{\pi(s_i, \Delta t)\}$	$\ldots \{\pi(s_i, \Delta t)\}\ P(S_i, t_0)$
p.8	$\ldots \underset{\sim}{Q}^+(s_i, \Delta t)\ \{\pi^1(s_{i+1}, t_0 + \Delta t)\}$	$\ldots \{\pi^1(s_{i+1}, t_0 + \Delta t)\}\ Q^+(s_i, \Delta t)$
p.8	$\ldots \underset{\sim}{Q}^-(s_i, \Delta t)\ \{\pi^2(s_{i-1}, t_0 + \Delta t)\}$	$\ldots \{\pi^1(s_{i-1}, t_0 + \Delta t)\ \ Q^-(s_i, \Delta t)$
p.9	$= \underset{\sim}{Q}^+(s_i, \Delta t)\ \{\pi^1(s_{i+1}, t)\}$	$= \{\pi^1(s_{i+1}, t)\}\ Q^+(s_i, \Delta t)$
p.9	$= \underset{\sim}{Q}^-(s_i, \Delta t)\ \{\pi^1(s_{i-1}, t)\}$	$= \{\pi^1(s_{i-1}, t)\}\ Q^-(s_i, \Delta t)$
p.13	$q^-_{jk}(s_k, t)$	$q^-_{jk}(s_i, t)$
p.24	in 100 yrs (Fig. 5.2)	at time = 100 yrs
p.24	Section of (Fig. 5.3)	Section A of (Fig. 5.3)
p.26	in 100 yrs	at time = 100 yrs
p.27	(Source 12A and 12B)	(Sections A and B)
p.30	in 138 yrs	at time = 138 yrs
p.30	137 yrs	138 yrs
p.32	Dependent Models (Fig. 5.9)	Dependent Model
p.34	8 ± 2	$8 \pm .2$
p.34	← Current Model $M_o = 8 \pm 2$, $t_o = 5$ yrs	← Current Model $M_o = 8 \pm .2$, $t_o = 30$ yrs
p.34		← Current Model $M_o = 8 \pm .2$, $t_o = 5$ yrs
p.35	$\Delta \ell$	Δs
p.37	$\Delta \ell$	Δs

1. INTRODUCTION

The objective of this study is to develop a probabilistic model for earthquake occurrences with temporal and spatial memory. Stochastic processes are used to characterize both the spatial and temporal dependencies of seismic occurrences along a fault. Currently, only homogeneous space and time transitions are considered. The resulting process however is evolutionary and depends on the specific sequence of events over a period of time. The model provides estimates on the cumulative activity of a fault over a future time period. In addition, probabilities of occurrences of individual events along a geologic fault at some specified future time are obtained when a descritized time scale is used. The information from these evaluations is particularly useful in engineering seismic hazard computations and for social and engineering seismic risk assessments.

The random nature of seismic occurrences and lack of understanding of their geophysical properties and mechanism justifies the use of stochastic processes for their modeling. Probabilistic models developed with the intent of representing the frequency and magnitude of earthquakes, have been based on the Poisson process (e.g., Cornell, 1968; Shah et al., 1974; Der Kiüreghian and Ang, 1975). The main assumptions in these models are that seismic events are independent in magnitude and occur independently in time and space. These assumptions contradict the observed temporal and spatial dependence, especially for large magnitude earthquakes. Some of the more recently developed models have attempted to represent clustering of earthquake occurrences in time (Shlien and

Toksoz, 1970; and Esteva, 1976). Other models have used strain energy release mechanisms (Hagiwara, 1975), ultimate strain mechanisms (Rikitake, 1975), and foreshock and aftershock sequences (Knopoff and Kagan, 1977). Spatial and temporal considerations for seismic events were included by Veneziano and Cornell (1974) in a general stochastic model and were applied to a simulation procedure. A semi-Markov model is used by Patwardhan et al. (1980) to describe the recurrence of great earthquakes based on the time between their occurrence. Each of these models represents some aspect of the earthquake phenomenon, but none consider all aspects collectively. In addition, some of the models are developed on the basis of specific regional data and are valid only for their corresponding locations.

The model proposed in this study is general and can be adopted to a variety of seismic regions. For some regions it may be desirable to use the space and time dependent model in conjunction with the Poisson model, the latter being applied to faults with relatively low magnitude events of uniform rate of occurrence. For demonstration purposes, the model is applied to two sections of the San Andreas fault, the Hayward fault and the Calaveras fault in California. For the two sections on the San Andreas fault, the model is compared to results obtained from the Poisson model of earthquake occurrences. In addition, forecasts for seismic activity off the shore of Alaska are obtained and compared to similar results reported by Patwardhan et al. (1980). Sensitivity analysis of the model is conducted to determine variations with time increments and space increments. Foreshock and aftershock sequences of

earthquakes can be represented with the current modeling approach by selecting the proper time increment for the model. This aspect of seismic occurrences is presently under investigation and is not included in this report.

2. MODEL DESCRIPTION

The sequence of large earthquake occurrences along a fault depends on the rate at which energy is accumulated along the fault and the capacity of the fault to retain this energy. Observations on past earthquake data reveal that considerable time elapses between major earthquakes. Traces of fault rupture after large earthquakes indicate that the total amount of energy released from such an earthquake emanated from a large area along the fault. In comparison, small magnitude events are believed to be due primarily to localized stress-strain concentration and redistribution (Nur, 1978). Consequently, when a more general energy-based mechanism is considered for modeling earthquake occurrences, the small magnitude events can be ignored.

In the current model, energy is assumed to accumulate at a constant rate, while the capacity to retain that energy varies along a geologic fault. Only slip-type linear faults are considered in this report. However, future extensions of the model will include thrusting faults and subduction zones, whose energy release mechanism and geometric configuration are more complex than those of slip faults.

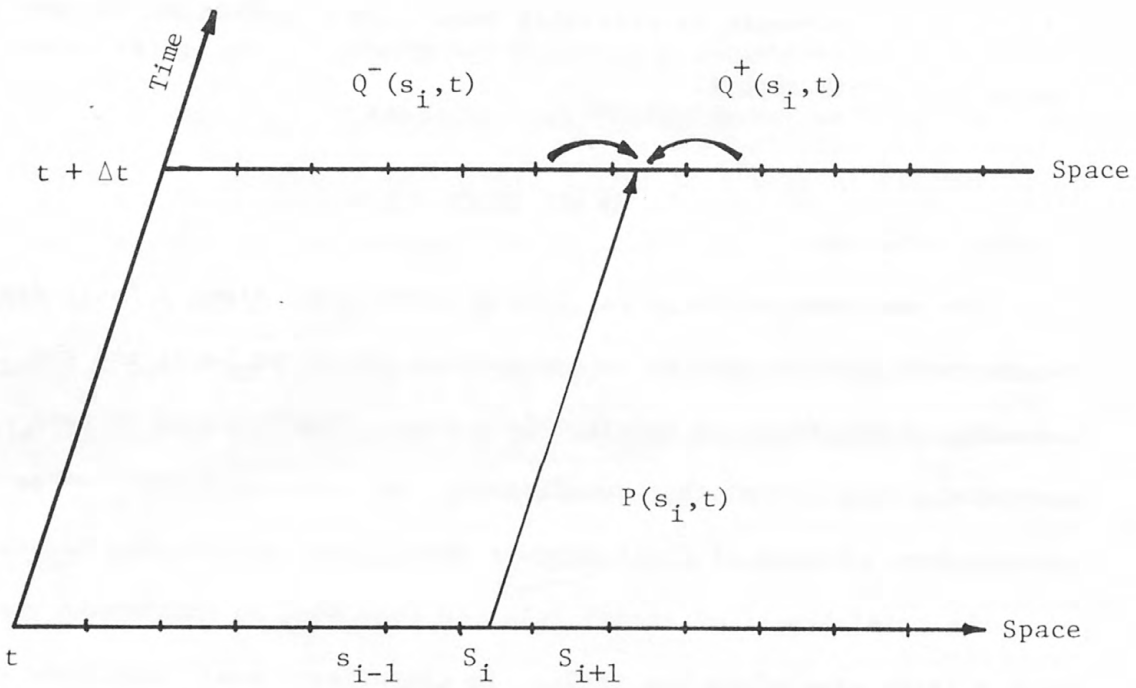

Figure 2.1 Time and space transition of process.

Figure 2.1 shows a linear fault of length L divided into equal segments of length Δs. The space coordinate is taken along the fault. The process is observed at every segment s_i along the fault as it progresses in time at increments of Δt. Discrete space, time and energy scales are used to enable the application of discrete models and to facilitate computations. At any time t, a segment s_i along the fault can release an amount of energy E_j, where E_j is the energy from a given size earthquake per unit length. The various levels of energy release form the state vector of the process denoted by

$$\{E_j\} = \{E_0, E_1 \ldots E_n\}$$

in which n is the number of different energy release values and E_0 denotes no energy release or release below some threshold values. The probability that an energy E_j is released at segment s_i at time t is given by $\pi_j(s_i,t)$. Then

$\{\pi(s_i,t)\}$ = state probability vector for segment s_i at time t

and the initial probability vector is

$\{\pi(s_i,t_0)\}$ = state probability vector for segment s_i at $t = 0$.

The process is observed as it moves from time t to $t + \Delta t$ at each segment s_i. During the time increment Δt energy release at segment s_i is related to activity at the same segment which occurred during the previous time increment. At the end of the time increment Δt, the influence of the fault segments adjacent to s_i is examined. These transitions are next discussed.

2.1 Time Transition

The probability that E_k amount of energy is released in time t to $t + \Delta t$ given that there was E_j energy released at segment s_i is denoted by $p_{jk}(s_i,\Delta t)$. The one step time transition matrix is given by

$\underset{\sim}{P}[s_i,\Delta t]$ = n x n matrix for segment s_i whose elements $p_{jk}(s_i,\Delta t)$ describe the probability of energy release of any E_k given that E_j was released in the previous time step.

The symbolic movement of the $\underset{\sim}{P}$ matrix is shown on Figure 2.1 for segment s_i. The matrix $\underset{\sim}{P}$ need not be the same for all segments along a fault and in general it is likely to differ over several portions of the fault. Currently only homogeneous time transition matrices are considered, i.e., the elements of $\underset{\sim}{P}$ are independent of the absolute time t. Possible time-dependent representations are presently under investigation.

2.2 Space Transition

At the end of the time t, segment s_i can have an energy release of E_k given that E_j energy was released at s_{i+1} at time t. The probability of that event occurring is denoted by $q^{+}_{jk}(s_i,\Delta t)$. The influence of the segment s_{i-1} on s_i is given by $q^{-}_{jk}(s_i,\Delta t)$. These probabilities form the elements of the space transition matrices.

$\underset{\sim}{Q}^{+}(s_i, t)$ = n x n matrix for probabilities of space transitions from segment s_{i+1} to s_i

and

$\underset{\sim}{Q}^{-}(s_i, t)$ = n x n matrix for probabilities of space transitions from segment s_{i-1} to s_i.

Segments at the end of the fault have only one-sided transitions.

2.3 Initial State Space

Since future energy releases depend on the previous energy releases, it is important to consider the time when the last major event occurred and the location where it occurred. Thus every segment along the fault is traced back in time to the latest major event that occurred on it. It is assumed that the process is renewed after each major event, i.e., energy accumulation starts from zero after every major event. The process is essentially started at each segment at the time of the most recent major event on that segment. If these times for the different fault segments are denoted by t_i^-, then the process for the overall fault is started from time $t_{max}^- = \max\{t_i^-\}$. At time $t^- = t_{max}^-$, segments which have no energy releases are assumed to start with a state probability vector $\{\pi(s_i, t_{max}^-)\} = \{1,0,0, \ldots, 0\}$. Generality is not lost by this assumption. When the process arrives at the time $t_i^- < t_{max}^-$ corresponding to the time of the last major occurrence for segment s_i, the state probability vector for s_i is reset to describe that energy release. For example, if at time t_i^- segment s_i had energy release of E_3 then the state probability vector is

$$\{\pi(s_i, t_i^-)\} = \{0,0,0,1,0 \ldots 0\}$$

in which $\pi_3(s_i, t_i^-) = 1$ and all other $\pi_i(s_i, t_i^-) = 0$. At time $t = t_0$ (the present), the process has reconstructed the recent history of major earthquakes along the fault.

2.4 Forecasting Process

Given that the process has been reconstructed to time $t = t_0$, forecasts are made on the basis of time and space transitions from one energy release level to another. At time $t_0 + \Delta t$, the transition in time alone is described by the time-state probability vector $\{\pi^1(s_i,t)\}$ and is obtained as follows:

$$\{\pi^1(s_i,t_0 + \Delta t)\} = \underset{\sim}{P}(s_i,t_0)\{\pi(s_i,\Delta t)\} \tag{1}$$

At the end of the time $t_0 + \Delta t$ the effect on segment s_i due to activity (or inactivity) at adjacent segments is found by the space transition probability matrices:

$$\{\pi^+(s_i,t_0 + \Delta t)\} = \underset{\sim}{Q}^+(s_i,\Delta t)\{\pi^1(s_{i+1},t_0 + \Delta t)\} \tag{2}$$

and

$$\{\pi^-(s_i,t_0 + \Delta t)\} = \underset{\sim}{Q}^-(s_i,\Delta t)\{\pi^1(s_{i-1},t_0 + \Delta t)\} \tag{3}$$

The state probability vector for s_i after one time and space transition is

$$\{\pi(s_i,t_0 + \Delta t)\} = \frac{1}{3}\left[\{\pi^1(s_i,t_0 + \Delta t)\} + \{\pi^+(s_i,t_0 + \Delta t)\} + \{\pi^-(s_i,t_0 + \Delta t)\}\right]. \tag{4}$$

In a similar manner, the state probability vector for segment s_i at some future time t is given by:

$$\{\pi(s_i,t)\} = \frac{1}{3}\left[\{\pi^1(s_i,t)\} + \{\pi^+(s_i,t)\} + \{\pi^-(s_i,t)\}\right] \tag{5}$$

in which

$$\{\pi^{+}(s_i,t)\} = \underset{\sim}{Q}^{+}(s_i,\Delta t)\{\pi^{1}(s_{i+1},t)\} \tag{6}$$

$$\{\pi^{-}(s_i,t)\} = \underset{\sim}{Q}^{-}(s_i,\Delta t)\{\pi^{1}(s_{i-1},t)\} \tag{7}$$

From equations 1 through 7, it can be observed that the process, in general, will depend on the initial probability vector and is evolutionary in time.

For engineering seismic risk analysis purposes it is important to obtain the cumulative probabilities of energy release over a time t. These are given by the vector $\{v(s_i,t)\}$ whose elements are determined in the recursive equation form:

$$\begin{aligned} v_j(s_i, 1) &= \pi_j(s_i, 1) \\ v_j(s_i, N) &= v_j(s_i, N-1) + [1 - v_j(s_i, N-1)] \\ &\quad [\sum_{k\neq j} \pi_k(s_i, N-1) P_{kj}(s_i, N-1) + \pi_j^{+}(s_i, N) \\ &\quad + \pi_j^{-}(s_i, N)]/3 \end{aligned} \tag{8}$$

in which

$$N = t/\Delta t \tag{9}$$

and $\pi_j^{+}(s_i, N)$ and $\pi_j^{-}(s_i, N)$ are as defined by Equations (6) and (7).

3. DEVELOPMENT OF TIME-TRANSITION MATRICES

The element $p_{jk}(s_i,t)$ of the time transition matrix $\underset{\sim}{P}(s_i,t)$ was defined as the probability of energy release of E_k at segment s_i in time t to $t + \Delta t$ given that there was an energy release of E_j at the same segment s_i at time t. A general statistical approach is considered for the determination of the $p_{jk}(s_i,t)$ values. Provided that sufficient data on time, location and magnitude of earthquake events is available, the homogeneous time-transition probabilities $p_{jk}(s_i,t)$ can be determined from:

$$p_{jk}(s_i,t) = \lim_{n_j \to \infty} \frac{n_{jk}}{n_j} \tag{10}$$

where

n_{jk} = the number of transitions from E_j to E_k

and

n_j = the total number of transitions from state E_j to any state E_k, i.e.,

$$n_j = \sum_{k=1}^{n} n_{jk} .$$

The time transition probabilities can also be related to the average time between events through the following

$$p_{jk}(s_i,t) = \frac{\Delta t}{T_{jk}} \tag{11}$$

where

Δt = time increment of process

T_{jk} = average time of transition from E_j to E_k.

Equation 11 is true provided that Δt is sufficiently small.

The average time between transitions, T_{jk}, is given by

$$T_{jk} = \lim_{n_{jk} \to \infty} \frac{1}{n_{jk}} \sum_{r=1}^{n_{jk}} T_{jk}^{r} \tag{12}$$

where T_{jk}^{r} = the time of the rth transition of the data from state E_j to state E_k.

For most seismic regions, however, the data is rather sparse and it is necessary to consider other sources of information in order to determine the probabilities $p_{jk}(s_i,t)$. For certain seismic faults, it is possible to estimate the average time between events from geologic or seismologic information. Bayesian statistical approach can be used to combine the various sources of information. In this approach, first a prior distribution with parameter θ is developed for the average time between events, denoted by $f'_{T_{jk}}(t_{jk}/\theta)$. The prior distribution $f'_{T_{jk}}(t_{jk}/\theta)$ is usually based on information from geologic or seismologic findings, or from historical, non-instrumentally recorded data. Instrumentally recorded data is employed to compute the likelihood function, $L(\theta/T_{jk}^{r})$. The posterior distribution on average time between events is given by (see Benjamin and Cornell, 1970)

$$f''_{T_{jk}}(t_{jk}) = N\, L\,(\theta/T^{r}{}_{jk})\; f'_{T_{jk}}(t_{jk}) \tag{13}$$

The transition probability $p_{jk}(s_i,t)$ is obtained using Equations (11) and (13) as follows:

$$p_{jk}(s_i,t) = \int_{o}^{\infty} \frac{\Delta t}{t_{jk}}\; f''_{T_{jk}}(t_{jk}) \tag{14}$$

Most often, the transition probability $p_{jk}(s_i,t)$ will be obtained from Equation (11) since in many cases it is difficult to obtain prior distributions for the transition times from E_j to E_k.

Another parameter which affects the transition probability $p_{jk}(s_i,t)$ is the time transition increment Δt. The selection of Δt must be such that no two transitions can occur within one time step. Yet the increment Δt should be large enough so that long term forecasts are computationally feasible. The size of the time increment, Δt, will affect the values of $p_{jk}(s_i,t)$ primarily for transitions to low energy release levels. The sensitivity of the model to variations in the increment Δt will be discussed further in Section 6 of this report.

With the assumptions stated in this section for the construction of the $\underset{\sim}{P}$ matrix and the assumptions for the $\underset{\sim}{Q}$ matrix to be described in Section 4; the time transition matrix, $\underset{\sim}{P}$, will have a dominant effect on the state probability vector and on the long term forecasts. It is of interest to observe that the model becomes a Markov chain when the transitions to various states are considered without the space dependence. For such a Markov process the steady state probabilities will always exist and the rate at which the steady state probabilities will be reached will depend on the average time between events. It is speculated that steady state probabilities will also be reached with the time and space dependent model. The rate at which these steady state probabilities are obtained will be investigated in Section 5.

4. DEVELOPMENT OF SPACE TRANSITION MATRICES

The elements $q^{+}_{jk}(s_i,t)$ and $q^{-}_{jk}(s_k,t)$ of the space transition matrices $\underset{\sim}{Q}^{+}(s_i,t)$ and $\underset{\sim}{Q}^{-}(s_i,t)$ were defined as the probabilities of energy release E_k at segment s_i given that the segment respectively from the right (s_{i+1}) or from the left (s_{i-1}) has an energy release of level E_j. Since the amount of energy released from a large earthquake will emanate from several segments along a fault, then the effect of one segment on an adjacent segment will depend on that energy release level and on the directivity of the rupture of the fault. For simplicity, it is assumed that an event originating at some segment along the fault will propagate the rupture in all directions along the fault with equal likelihood. This assumption of equal likelihood of all directions of rupture is conservative considering the present state of knowledge. If the directivity of a fault section is known, it can be easily incorporated in the computations of $\underset{\sim}{Q}^{+}$ and $\underset{\sim}{Q}^{-}$.* The transitions from the left for $\underset{\sim}{Q}^{+}$ and from the right for $\underset{\sim}{Q}^{-}$ are developed separately as described in the following paragraphs.

In general, if a fault is of length L and the rupture length l_j corresponding to an earthquake with energy release level E_j per unit length, the number of fault rupture segments u_j in l_j is:

$$u_j = l_j/\Delta s \tag{15}$$

in which Δs is the length of one segment.

*If small enough increments Δs and a finer energy release scale is used, then foreshock and aftershock sequences can be represented through the formulation of the $\underset{\sim}{Q}^{+}$ and $\underset{\sim}{Q}^{-}$ matrices.

Let U denote the total number of segments in the fault of length L, which is

$$U = L/\Delta s. \tag{16}$$

Two cases are identified in the construction of each of the Q^+ and Q^- matrices, depending on the relationship between the total number of segments in a fault, U, and the number of fault rupture segments u_j.

Consider the formulation of the Q^+ matrices:

Case a: For $u_j > U/2$ and

(i) segments $i = 1,2, \ldots, U - u_j$

$$q^+_{jj} = \frac{i}{i+1} \tag{17a}$$

$$q^+_{jk} = \frac{1}{j} \cdot \frac{1}{i+1}, \quad k = 0,1,2, \ldots, j-1; \tag{17b}$$

(ii) segments $i = U - u_j + 1, U - u_j + 2, \ldots, U$

$$q^+_{jj} = 1.0 \tag{17c}$$

$$\text{all other } q^+_{jj} = 0. \tag{17d}$$

Case b: For $u_j \leq U/2$ and

(i) segments $i = 1,2,3, \ldots, u_j - 1$

$$q^+_{jj} = \frac{1}{i+1} \tag{18a}$$

$$q^+_{jk} = \frac{1}{j} \cdot \frac{1}{i+1}, \quad k = 0,1,2, \ldots, j-1; \tag{18b}$$

(ii) segments $i = u_j, u_j + 1, \ldots, U - u_j$

$$q^{+}_{jj} = \frac{u_j - 1}{u_j} \tag{18c}$$

$$q^{+}_{jk} = \frac{1}{j} \cdot \frac{1}{u_j}, \quad k = 0,1,2, \ldots, j-1 \; ; \tag{18d}$$

(iii) segments $i = U - u_j + 1, U - u_j + 2, \ldots U$

$$q^{+}_{jj} = 1.0 \tag{18e}$$

and all other $q^{+}_{jk} = 0.$ (18f)

The expression for q^{+}_{jk} is obtained by assuming that the segment beyond the last segment of rupture has equal probability of releasing energy of value $E_{j-1}, E_{j-2}, \ldots E_0$. This assumption is based on the hypothesis that at the ends of a rupture zone there will be stress concentration and the segments immediately adjacent to the rupture zone can have an amount of energy released smaller than the energy per segment released along the ruptured portion. This smaller amount of energy includes also zero energy release, i.e., E_0. The same assumption is made in the construction of the elements of the $\underset{\sim}{Q}^{-}$ matrix.

Consider the formulation of the $\underset{\sim}{Q}^{-}$ matrix:

Case a: For $u_j > U/2$ and

(i) segments $i = 1,2,3, \ldots, u_j$

$$q^{-}_{jj} = 1.0 \tag{19a}$$

(ii) segments $i = u_j + 1, u_j + 2, \ldots, U$

$$q^{-}_{jj} = \frac{U - i + 1}{U - i + 2} \tag{19b}$$

$$q^{-}_{jk} = \frac{1}{j} \cdot \frac{1}{U - i + 2} \qquad k = 0,1,2, \ldots, j-1 \tag{19c}$$

and all other $q^{-}_{jk} = 0$ (19d)

Case b: For $u_j \leq U/2$ and

(i) segments $i = 1,2,3, \ldots, u_j$

$$q^{-}_{jj} = 1.0 \tag{20a}$$

(ii) segments $i = u_j + 1, u_j + 2, \ldots, U - u_j + 1$

$$q^{-}_{jj} = \frac{u_j - 1}{u_j} \tag{20b}$$

$$q^{-}_{jk} = \frac{1}{j} \cdot \frac{1}{u_j}, \qquad k = 0,1,2, \ldots j-1; \tag{20c}$$

(iii) segments $i = U - u_j + 2, U - u_j + 3, \ldots, U$

$$q^{-}_{jj} = \frac{U - i + 1}{U - i + 2} \tag{20d}$$

$$q^{-}_{jk} = \frac{1}{j} \cdot \frac{1}{U - i + 2} \quad k = 0,1,2, \ldots, j-1; \tag{20e}$$

and all other $q^{-}_{jk} = 0.$ (20f)

In all cases, $q^{\pm}_{jj}$ are obtained by considering the number of ways a rupture of length u_j (or ℓ_j) can be at both segments s_i and s_{i+1} or s_{i-1}, normalized to the number of ways the rupture can cover only segment s_{i+1} or s_{i-1}, respectively.

Another aspect of fault rupture which can be incorporated in the formulation of the $\underset{\sim}{Q}^{+}$ and $\underset{\sim}{Q}^{-}$ matrices is the uncertain nature of the fault rupture vs. energy relationship. This will require knowledge of the probability distribution of fault rupture length for a given energy release level. Then the formulas in equations (17) to (20) for each q_{ij} will represent conditional probabilities given the fault rupture length. To obtain q_{jk} then it is necessary to consider

$$q^{\pm}_{jk} = \sum_{\nu} P[E_k(s_i)/E_j(s_{i\pm1}), \ell_\nu] \; P\,[\ell_\nu/E_j(s_{i\pm1})]. \tag{21}$$

Most often the dispersion of the fault rupture vs. energy release is not well known and the assumption on the form of distribution for $P[\ell/E]$ remains rather arbitrary. It was felt that the inclusion of this arbitrary distribution will not contribute considerably to the model formulation while introducing another complication in the overall formulation. Consequently, it was not included in the application.

5. SEISMIC HAZARD OF THE SAN FRANCISCO BAY AREA

In order to test the stochastic time and space dependent model developed in this study, several faults in the San Francisco Bay Area were selected. The faults in this region which would generate earthquakes with significant hazard potential are the San Andreas, Hayward and Calaveras. The study region and the selected faults are identified in Figure 5.1. Within the San Andreas fault, two different patterns in frequency and magnitudes have been observed (Kiremidjian and Shah, 1975). Activity in the northern half of the fault, identified in Figure 5.1 as Section A, is characterized by the 1906 San Francisco earthquake of magnitude 8.3 and by very few events in the magnitude range from 4.0 to 8.3. In contrast, in the southern half of the fault, labeled in Figure 5.1 as Section B, activity is dominated by numerous small and medium size earthquakes, the largest of which reaches a magnitude of 6.5 In addition, some creeping motion has been associated with Section B of the San Andreas. This distinction in the rates of activity in the two sections of the San Andreas is reflected in the model by considering different time-transition matrices for the two segments. The Hayward and Calaveras faults have very similar activity rates and are geographically located very closely to each other. Consequently, they are modeled as a single line source with frequency of occurrences typical to both faults.

Information on the activity of each of the study faults was based on past earthquake occurrence data. Instrumentally recorded data from 1906 to 1976 were obtained from the National Earthquake Information

Center, Boulder, Colorado. These data contain information on magnitude, epicentral location, time of occurrence and focal depth for most of the recorded seismic events. Historical data from 1800 to 1906 were also reviewed. These data contain information primarily on the intensity of the event and the general region of occurrence. Additional insight on the average time between very large events was gained through reports from carbon dating of past occurrences on the San Andreas fault. (Cotton et al., 1980). Strain accumulation rates (Scholtz and Fitch, 1969; Savage and Burford, 1973; Thatcher, 1975a, 1975b) and rates of creep (Steinbrugge et al., 1960) were also reviewed and were used only in developing a general understanding of the behavior of the study faults.

The selection of the energy scale for the state space vector, $\{E\}$, the time increment, Δt, and the space increment, Δs, depends on the assumptions in the model and the availability of data. Furthermore, amount of energy release, time of release and rupture length are related and their dependence must be considered in the selection of ΔE, Δt and Δs. Various measures have been used to represent earthquake energy release. Among these, the most widely used ones are the Richter magnitude, M, shear wave magnitude, M_s, and body wave magnitude M_b. The majority of the past earthquake occurrence data are reported in terms of one of the magnitude values. Another measure which has been employed in recent years is the seismic moment, M_o. However, only a small fraction of the seismic data are reported in terms of seismic moment. Several relationships between seismic moment and various magnitude scales have been reported (e.g., Hanks and Kanamori, 1979; Percaru and Berckhemer, 1978; Thatcher and Hanks,

1973). The use of these relationships in converting reported magnitude values to seismic moments cannot be justified because of the large scatter around these relationships. The scatter is greatest for large magnitude events. Since most of the data are reported in one of the magnitude scales, and widely accepted relationships between the various magnitudes scales exist, the Richter magnitude is selected as the parameter for the model. It should be noted, however, that any one of the magnitude scales, or seismic moment can just as easily be applied with this model, provided the necessary data are available.

The faults considered in the application of the model are discretized into segments of Δs equal to 5 km. This Δs corresponds to earthquake rupture resulting from an event with an approximate magnitude equal to 6.0. Thus only events with magnitudes greater than or equal to 6.0 are considered. Since a discrete state space $\{E\}$ is used in the model, the magnitude scale is discretized into increments of 0.5, starting at a magnitude of 6.0 Due to the uncertainty in recording earthquake magnitudes, however, an increment of 0.25 or smaller for the magnitude scale is considered unrealistic. Thus, a $\Delta m = 0.5$ is felt to be consistent with the uncertainties in the data and minimizes computational difficulties.

The selected time step, Δt, is a one year interval. For magnitude 6.0 and larger earthquakes, the likelihood of observing two or more events within the same year is very small, thus a Δt of one year appears to be reasonable. The size of Δt is also governed by the smallest transition time between events. After a review of these

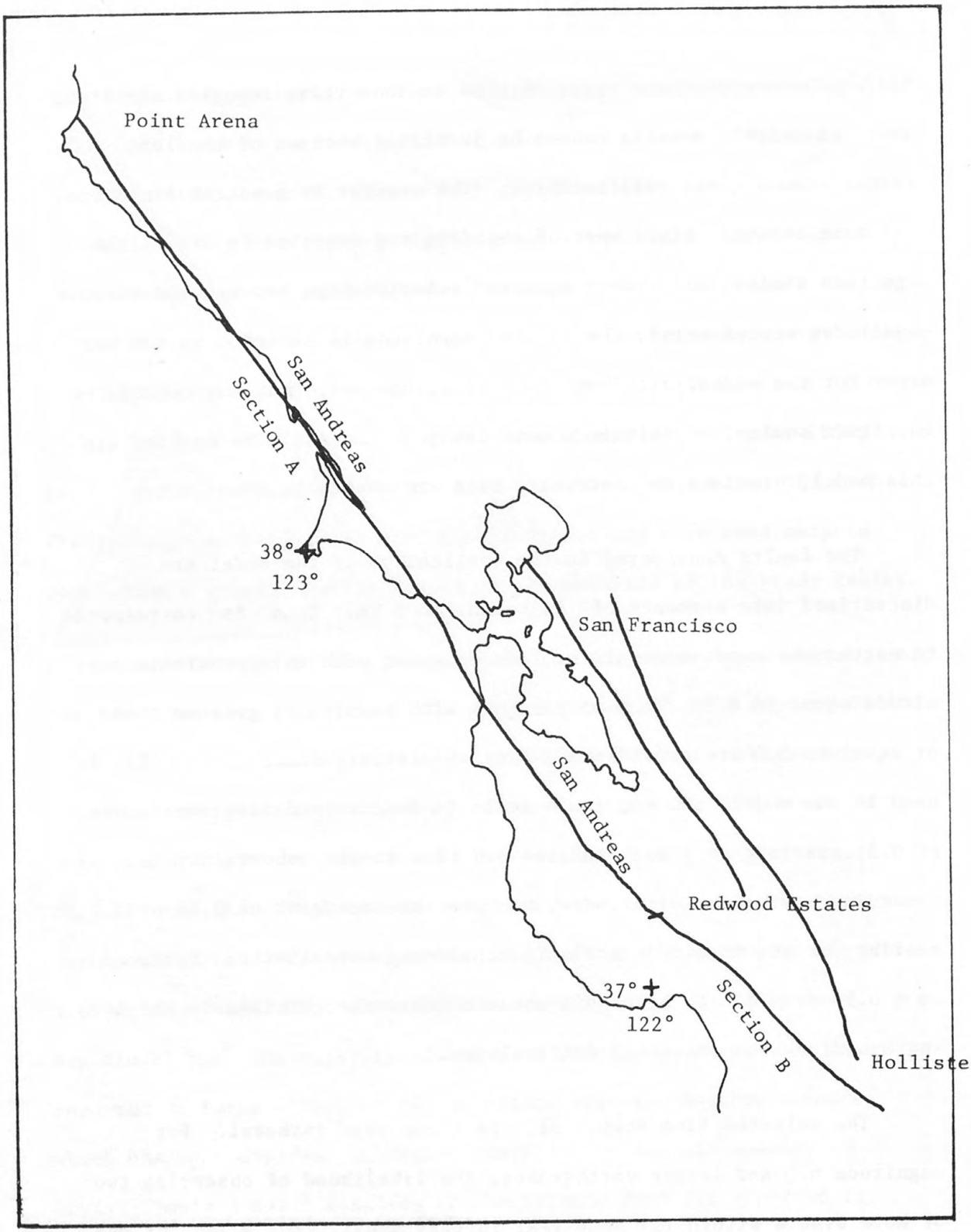

Figure 5.1 Study section: San Francisco Bay Area with major faults.

transition times, it was further affirmed that a Δt of one year is a reasonable choice. A three-year time increment was also used for sensitivity analysis purposes and the results from these computations will be discussed later in this section.

Table 5.1. Relationship Between Magnitude, Fault Rupture and Energy Release (After Slemmons, 1978)

M	ℓ (km)	E (ergs)	$E/\Delta\ell$	$u_j = \ell/\Delta\ell$
6.0	3.2	6.3×10^{20}	1.3×10^{20}	~ 1
6.5	7.2	35.5×10^{20}	7.1×10^{20}	~ 2
7.0	16.6	2.0×10^{22}	4.0×10^{21}	~ 4
7.5	39.1	11.2×10^{22}	2.2×10^{22}	~ 8
8.0	91.4	63.1×10^{22}	1.3×10^{23}	~19
8.5	214.4	35.5×10^{23}	7.1×10^{23}	~43

To gain further insight into the problem, the energy, fault rupture, and magnitude relationship is studied for the magnitude range of interest (after Slemmons, 1978). Table 5.1 shows the amount of energy released per 5 km segment and the approximate number of segments ruptured from a given magnitude earthquake. The energy levels E_j, are then defined in units of 10^{20} ergs as:

$E_0 < 1.3$ $\quad$ $E_4 = 220.0$

$E_1 = 1.3$ $\quad$ $E_5 = 1300.00$

$E_2 = 7.1$ $\quad$ $E_6 = 7100.00$

$E_3 = 40.0$

With the above definitions of $\{E\}$, Δt, $\Delta \ell$, and denoting the lengths of Sections A and B of the San Andreas by L_1 and L_2, respectively, tests on the model were conducted with initial conditions starting at magnitude 8.3 in 1906 and retracing the magnitude 6.0 and greater earthquakes at more recent times. The space transition matrices for both Sections A and B were developed on the basis of the u_j values from Table 5.1 and U = 65. The space transition matrices for both Sections A and B are taken to be the same because of the continuity of the fault from segment A to segment B. (In the 1906 San Francisco earthquake, the fault rupture extended over parts A and B). Time transition matrices are developed from the average times between events shown in Tables 5.2 and 5.3 (The values shown in parenthesis are assumed values and are not based on data observation).

Table 5.2. Average Time Between Energy Releases for San Andreas Segment A. (Values in parenthesis are assumed.)

From \ To	E_1	E_2	E_3	E_4	E_5	E_6
E_0	(14)	(20)	(30)	(50)	(70)	(90)
E_1	15	30	(45)	(60)	(80)	(100)
E_2	15	30	(60)	(80)	(100)	(120)
E_3	(20)	(35)	60	(100)	(150)	(180)
E_4	(20)	(40)	(70)	110	(150)	(180)
E_5	(20)	(40)	(80)	(120)	160	(200)
E_6	20	(50)	(90)	(150)	(180)	300

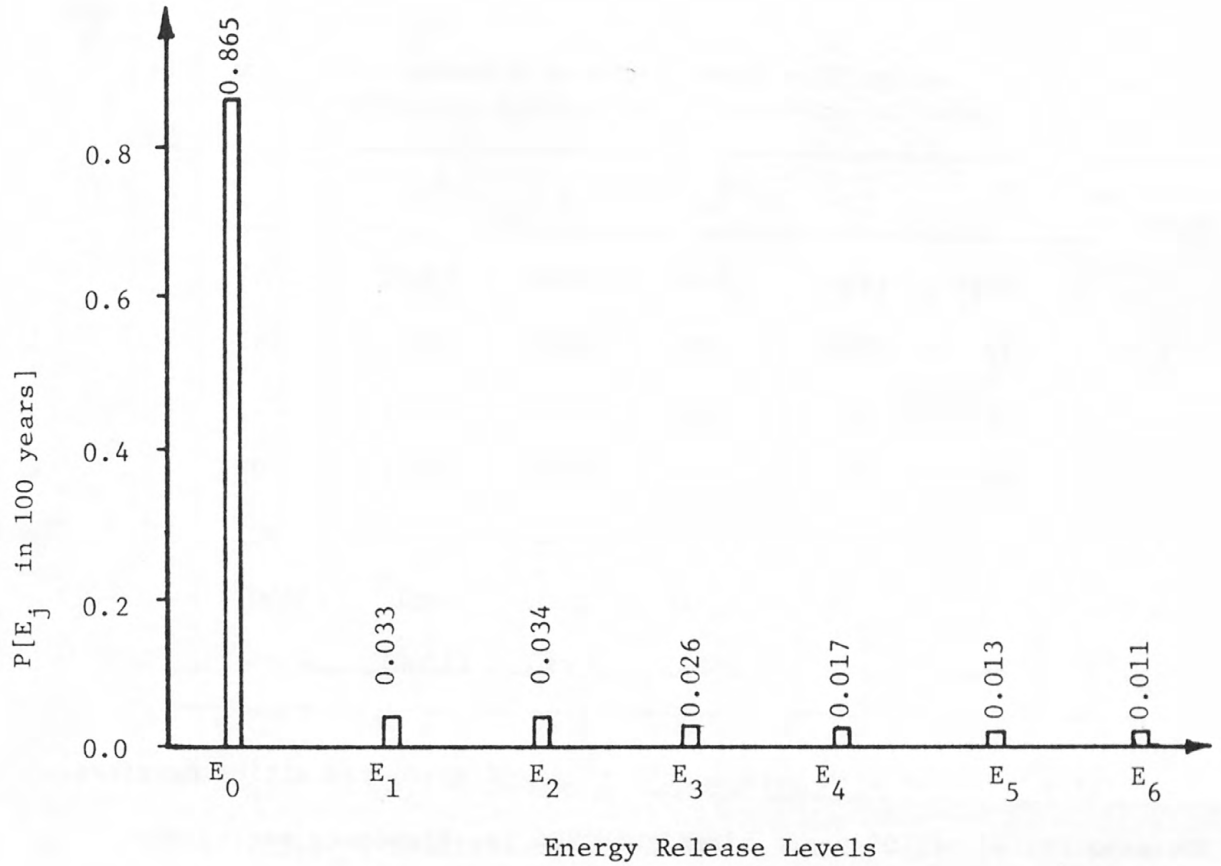

Figure 5.2 Probabilities of releasing energy E_j in 100 years since the last major event on Section A of the San Andreas fault.

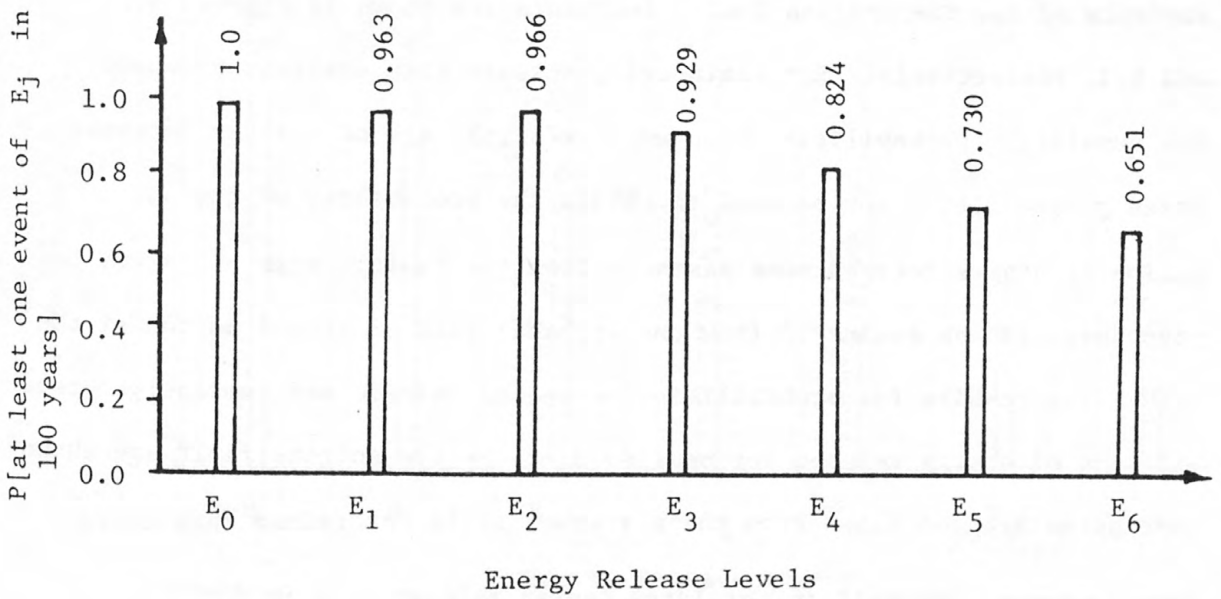

Figure 5.3 Probabilities of at least one event of E_j in 100 years since the last major event on Section of the San Andreas fault.

Table 5.3. Average Time Between Energy Releases for San Andreas Segment B. (Values in parenthesis are assumed.)

From \ To	E_1	E_2	E_3	E_4	E_5	E_6
E_0	(21)	(58)	(150)	(200)	(300)	(400)
E_1	22	(30)	(70)	(225)	(350)	(425)
E_2	(30)	59	(90)	(250)	(400)	(1000)
E_3	(20)	(80)	154	(300)	(600)	(2000)
E_4	(15)	(100)	(250)	408	(700)	(2500)
E_5	(10)	(100)	(275)	(450)	1081	(3000)
E_6	(8)	16	(300)	(500)	(1000)	4608

Tests were run with homogeneous time and space transition matrices for time period of 100 years after the 1906 San Francisco earthquake. The probabilities of releasing energy E_j in time t, $\pi_j(s_i,t)$, and probabilities of at least one E_j in time t, $v_j(s_i,t)$, for central segments of the San Andreas fault, Section A are shown in Figures 5.2 and 5.3, respectively. For engineering seismic risk analysis purposes, the cumulative probabilities of events $v(s_i,t)$ are of greater interest. These probabilities can be used to obtain the probability of ground motion at a site located some distance from the fault. Risk of damage to structures can be evaluated from the probabilities of ground motion at the site. The results for probabilities of energy release and cumulative probabilities of energy release for Section B of the San Andreas fault are shown in Figures 5.4 and 5.5. From these graphs, it is determined that considerably lower probabilities of large energy releases are obtained on Section B than on Section A, which is consistent with actual observations. Figure 5.6 shows the probabilities of at least one E_4, E_5

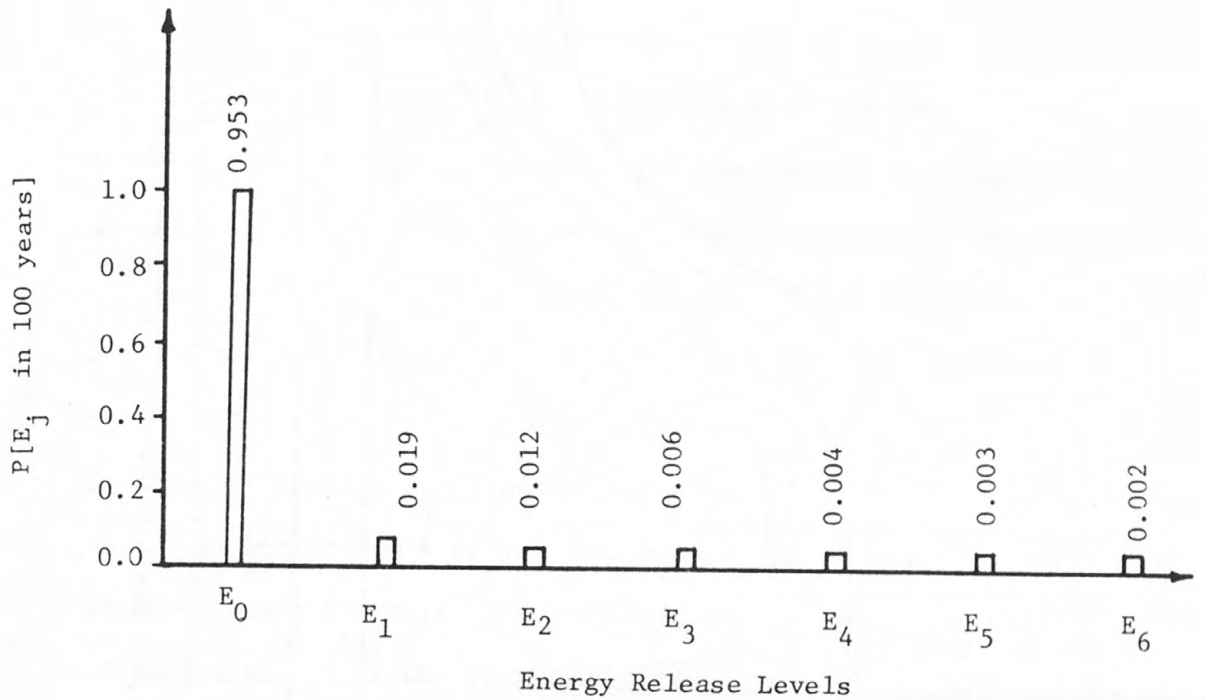

Figure 5.4 Probabilities of releasing energy E_j in 100 years since the last major event on Section B of the San Andreas fault.

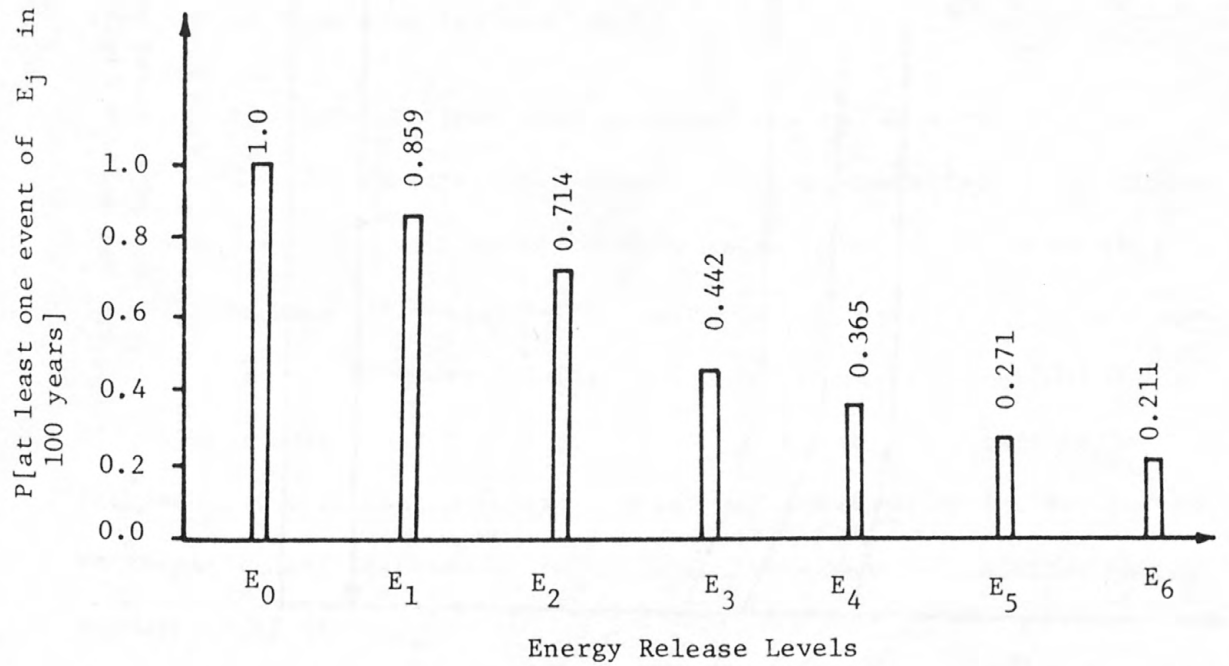

Figure 5.5 Probabilities of at least one event of E_j in 100 years since the last major occurrence on Section B of the San Andreas fault.

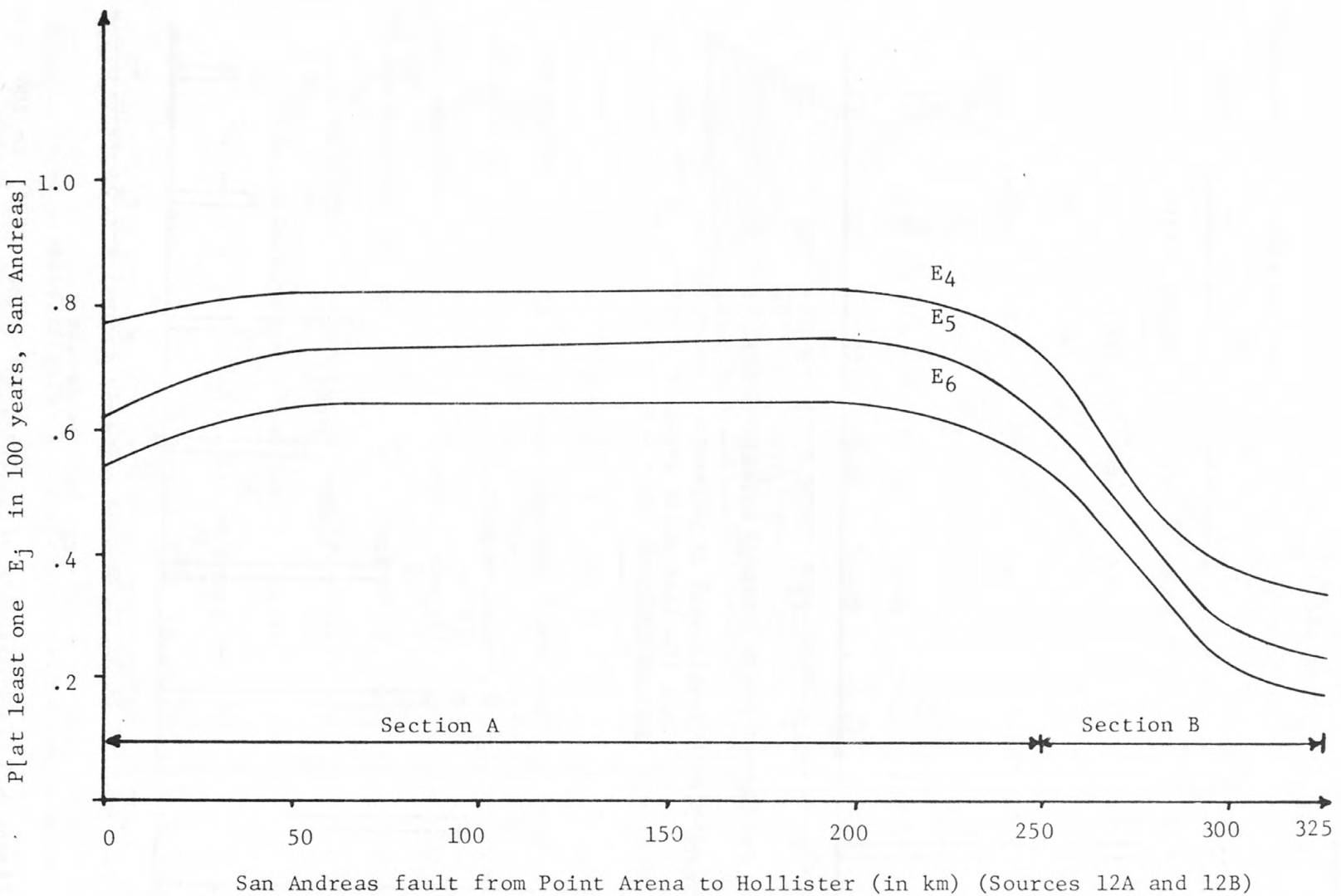

Figure 5.6 Probabilities of at least one Ej in 100 years since the last major event along the San Andreas fault.

and E_6 as a function of the distance along the fault. The decrease in probabilities for large E_j's in Section B of the fault can be seen explicitly in this chart. The effect of the spatial dependence of the model can be observed in the increased probabilities of occurrence of at least one E_j in the range of Section B which is closest to Section A. A probability of 0.651 for at least one earthquake of E_6 ($M \approx 8.5$) since the last major event appears to be reasonable for San Andreas Section A. A probability of 0.211 for at least one E_6 ($M \approx 8.5$) on Section B of San Andreas appears to be rather high. The primary reason for this large value is the influence of Section A, as already stated. In the course of these tests, it was also observed that steady state probabilities for E_j were reached only after a few time steps. The steady state probabilities were obtained just as fast for Section A as for Section B.

Similar computations were performed for the Hayward-Calaveras fault zone. The average time between events on these faults are listed in Table 5.4. The last major event on these faults occurred in 1868. In order to make a forecast to the year 2006 to coincide with the computations for the San Andreas fault, the time period from the last event to the year 2006 was taken as 138 years. Based on the total length of the fault, the largest magnitude event that can occur on the Hayward and Calaveras faults is taken as 7.5. This corresponds to a maximum energy release level of E_4.

Table 5.4. Average Time Between Energy Releases for Hayward-Calaveras Faults (Values in parenthesis are assumed.)

From \ To	E_1	E_2	E_3	E_4
E_0	(25)	(65)	(90)	(160)
E_1	50	(80)	(125)	(250)
E_2	(55)	117	(220)	(375)
E_3	(60)	(130)	275	(500)
E_4	(65)	(150)	(400)	647

Probabilities of energy release E_j in time t, $\pi_j(s_i,t)$, and of at least one energy release of level E_j in time t, $v_j(s_i,t)$, are shown in Figures 5.7 and 5.8, respectively. The probability values in these figures are even lower than corresponding values for the San Andreas Section B. This is also consistent with actual observations, since primarily small and medium size events are characteristic of these faults. Thus, for the overall San Francisco Bay Area, the major source of large earthquake events as predicted by the model is the northern section of the San Andreas fault, followed by Section B of the San Andreas and by the Hayward-Calaveras fault zone.

Previous studies based on the Poisson model of earthquake occurrences have made the same predictions as described in the previous paragraph. It is of interest to compare the results obtained from the space and time dependent model to the results from the simple Poisson model. This comparison for probabilities of at least one event of energy release level E_j or greater than E_j for Section A of the

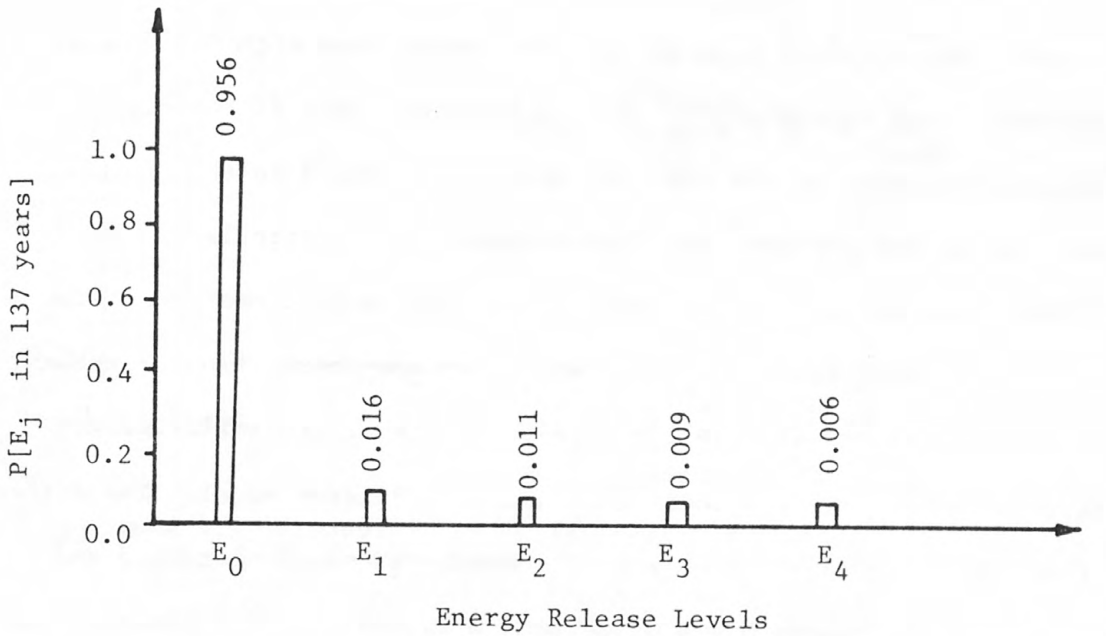

Figure 5.7 Probabilities of releasing energy E_j in 138 years since the last major event on the Hayward-Calaveras fault zone.

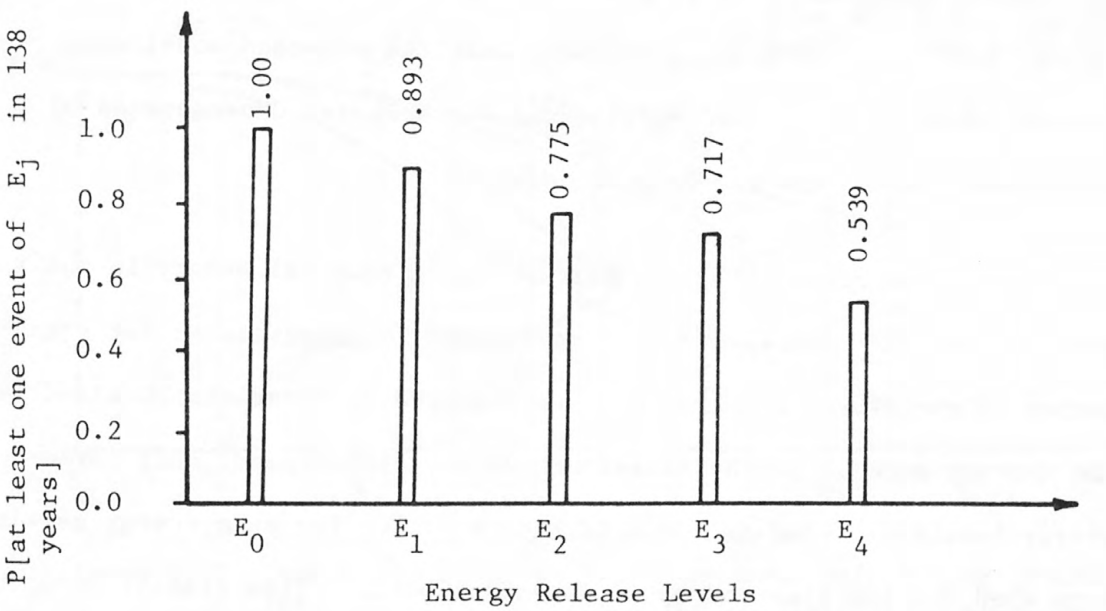

Figure 5.8 Probabilities of at least one event of E_j in 138 years since the last major event on the Hayward-Calaveras fault zone.

San Andreas fault is shown on Figure 5.9. Lower probabilities of occurrence are obtained with the proposed model than with the Poisson model when large values of E_j are considered. This difference is to be expected because of the time dependence introduced in the current model. As stated earlier, the time dependence is particularly important for large energy release levels. When the same comparison between the proposed model and the Poisson model is made for Section B of the San Andreas (see Figure 5.10), considerably higher probabilities are observed with the current model than with the Poisson model. The difference in probability values increases in the northern end of Section B and it decreases as the southern end of Section B is approached. Clearly, the spatial dependence of the current model causes this increase in probabilities near Section A. Independence both in time and space is assumed for the Poisson model and thus it predicts the same probability values throughout the fault. It is felt, therefore, that the proposed model more realistically represents both the spatial and the temporal dependencies of earthquake events than the Poisson model.

Patwardhan et al. (1980) considered only temporal memory in their semi-Markov model for earthquake occurrences. Their results for earthquakes in the circum-Pacific belt are compared to forecasts obtained from the current model. In the Patwardhan et al. (1980) paper only three energy levels are used as shown in Figure 5.11. The same energy levels were used for the time and space dependent model. Time transition probabilities were based on data provided by the Patwardhan et al. (1980) paper. These data were for a very large region and could not be associated with

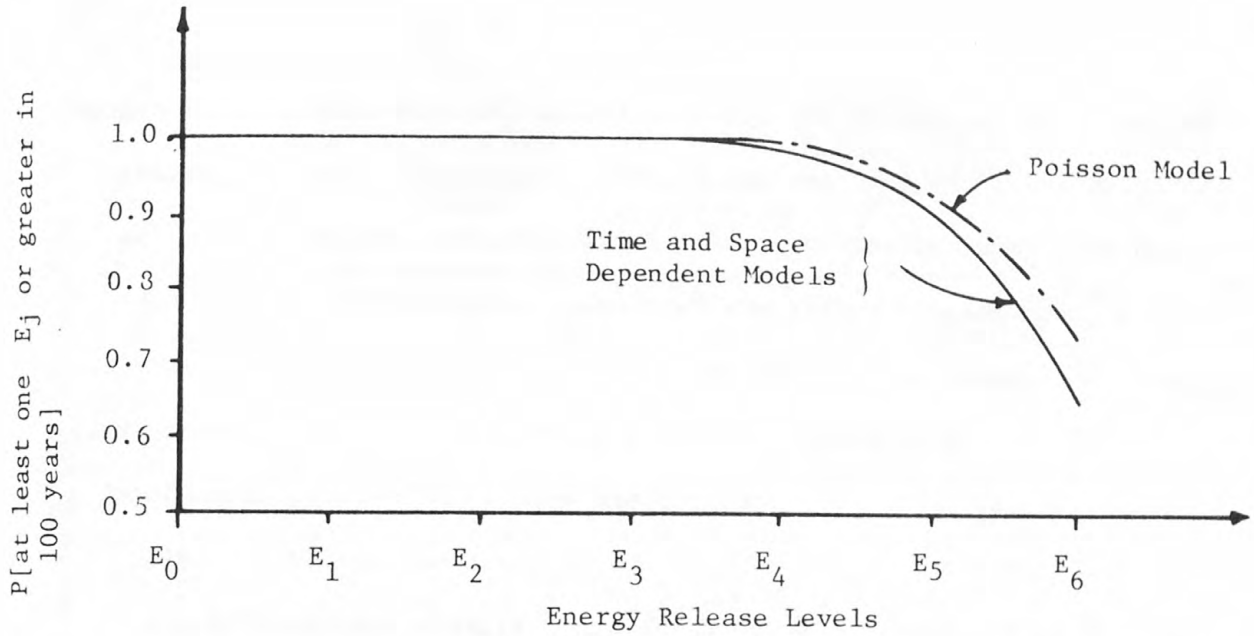

Figure 5.9 Probabilities of at least one event of E_j or greater than E_j in 100 years since the last major event on Section A of the San Andreas fault using the Poisson model and the time and space dependent model of this report.

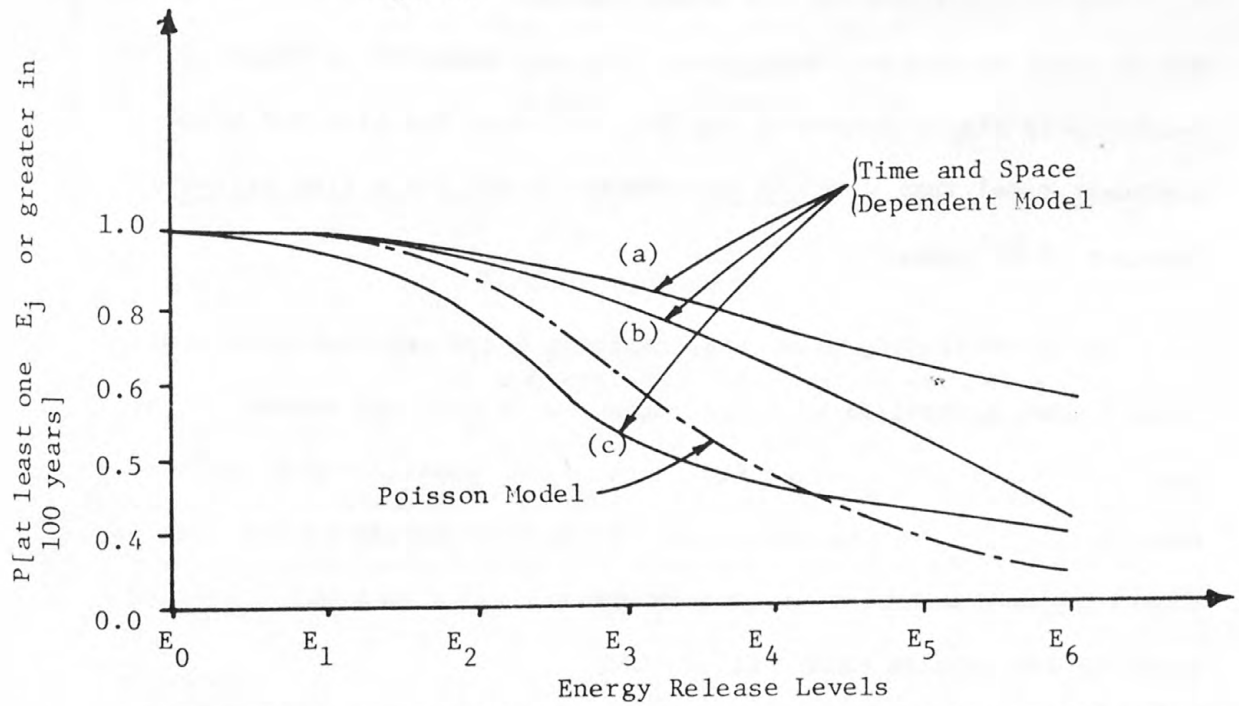

Figure 5.10 Probabilities of at least one event of E_j or greater than E_j in 100 years since the last major event on Section B of the San Andreas fault using the Poisson model and the time and space dependent model. The three curves for the time and space dependent model correspond to (a) northernmost segments of Section B; (b) central segments of Section B; (c) southernmost segments of Section B.

the activity pattern of any specific fault. Because such a large region is considered, the data contained many earthquakes of large magnitudes which have occurred within a short period of time. Consequently, the average time between events are very small resulting in large probabilities of transitions. It is recognized that with such large transition probabilities the forecasts on earthquake occurrences are expected to be greatly overestimated with the proposed model. More detailed regional information on earthquake activity and on the temporal and spatial patterns is necessary in order to obtain realistic results with the current model. The analysis for the circum-Pacific belt, however, is considered only for comparison purposes. Space transition probabilities could not be developed for the study region. The results from the two models based on temporal dependence only are compared in Figure 5.11. Considerably higher forecasts are obtained with the time and space dependent model than with the semi-Markov model for a time period of forecast of 40 years.

It is concluded, therefore, that the space and time dependent model cannot be applied to large regions with diffused seismic information. This model requires knowledge of the behavior of a fault or a fault zone. Results obtained on local regional models rather than on global regional model are of greater use and value in earthquake risk analysis and seismic hazard mitigation.

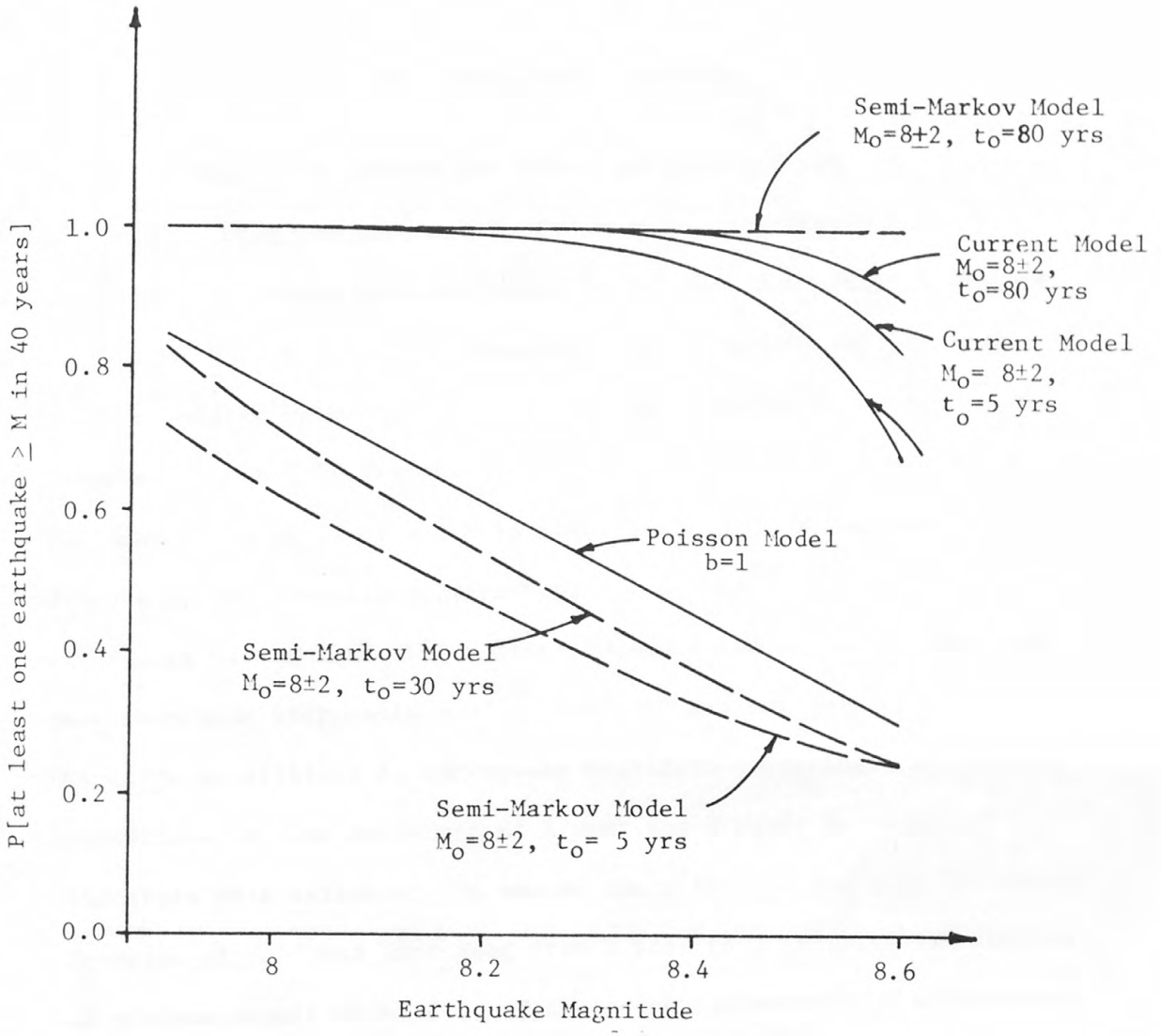

M_o, t_o initial conditions
M_o = magnitude of last great earthquake
t_o = waiting times since the last great earthquake

Figure 5.11 Comparison of probabilities of at least one event ≥ M in 40 years on the circum-Pacific belt using the semi-Markov, the time and space dependent model and the Poisson model

6. SENSITIVITY ANALYSIS

In order to determine the effect of the different parameters on the results from the time and space dependent stochastic model, sensitivity analyses were performed on the time and space parameters. The sizes of time and space increments are functions of the minimum value of energy release, E_j, as well as of energy release increments, ΔE. It was decided in Section 5 of the report that the lowest energy level which is significant for spatial and temporal dependence representation corresponds to the energy released from an earthquake of magnitude 6.0. It was also stated earlier in the report that magnitude increments smaller than 0.5 are not justified because of the large uncertainty in earthquake magnitude reporting. With these assumptions, a time increment of 1 year and a space increment of 5 kilometers were selected. To assess the effect of the time increments, the value of Δt was increased from 1 year to 3 years, while keeping the minimum magnitude at 6.0 and the space increment at 5 kilometers. The probability of two or more events in a three-year period is still relatively small so that the major assumptions in the model are not violated. If a larger time increment were selected, then the minimum magnitude and consequently the lowest energy release level would have to be increased to comply with the assumption of small probability of two or more events in a Δt. An increase in E_{min} would require also an increase in $\Delta \ell$. For a Δt of 3 years, $\Delta \ell$ of 5 km and lowest

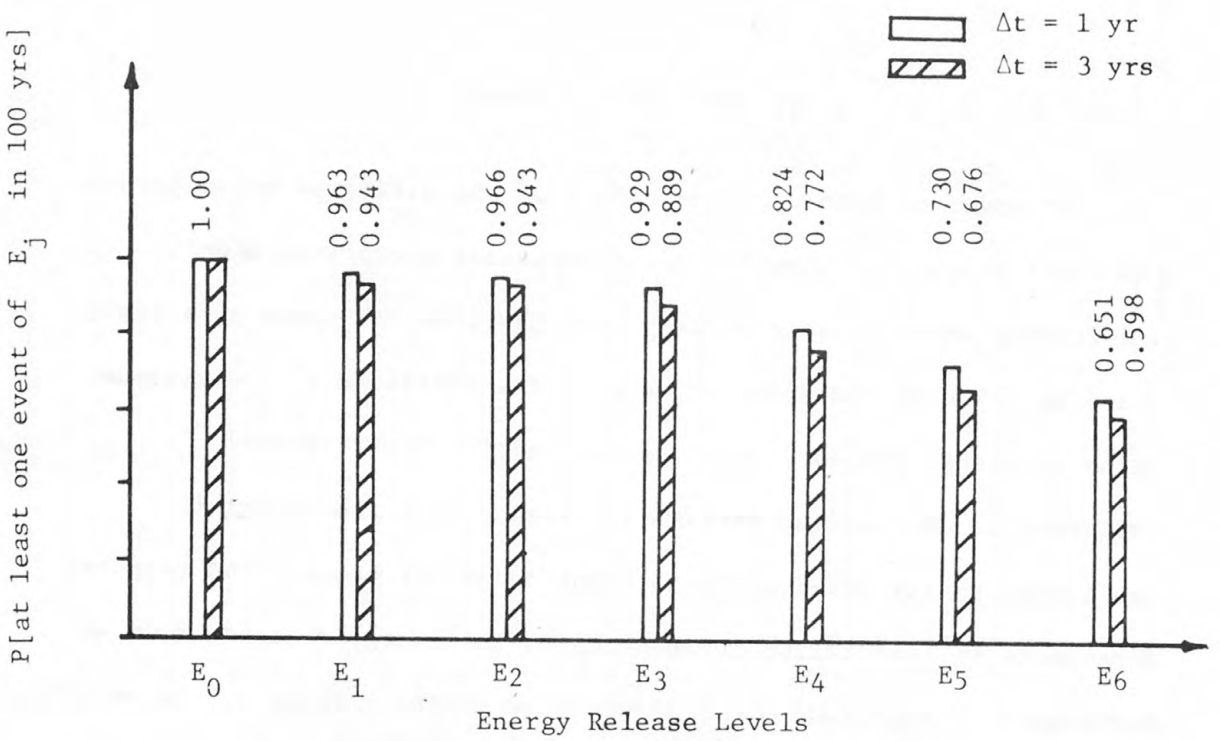

Figure 6.1 Probabilities of at least one event of E_j in 100 years since the last major event on Section A of the San Andreas fault using 1 year and 3 year time increments.

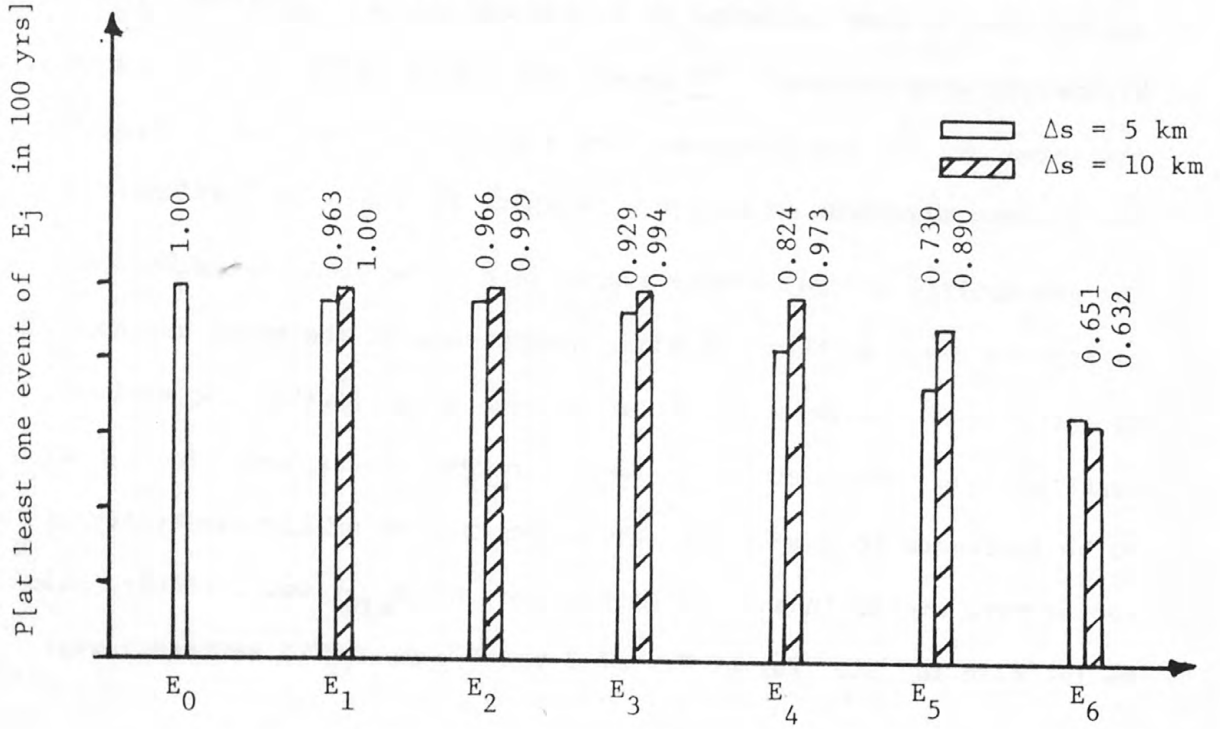

Figure 6.2 Probabilities of at least one event of E_j in 100 years since the last major event on Section A of the San Andreas fault using space increments of 5 km and 10 km.

energy release level corresponding to magnitude of 6.0, the probabilities for at least one E_j on Section A of San Andreas fault are shown in Figure 6.1. Slightly lower probabilities are obtained with Δt of 3 years than with Δt of 1 year. This difference is less than one percent at the highest energy release level, and is not considered to be significant. The primary reason for the decrease in probabilities with increased Δt is that fewer time steps are necessary to reach the 100 years since the last event, which decreases the rate at which energy is accumulated at the fault. A time increment of 1 year with the choice of E_{min} corresponding to magnitude 6.0 and $\Delta \ell$ of 5 km appears to be reasonable and fairly stable.

The second sensitivity test was concerned with the space increment $\Delta \ell$. If a $\Delta \ell$ of 10 km is used, then the minimum energy release level is fixed at a magnitude of 6.5. The time and space transition matrices were corrected for that E_{min} value. The assumption of a one year time increment is still valid and does not need an adjustment. The results from this test are shown in Figure 6.2. The comparison of the graphs for $\Delta \ell$ of 5 km and $\Delta \ell$ of 10 km on the San Andreas Section A show that the probabilities are only slightly higher for $\Delta \ell$ of 10 km than the values for $\Delta \ell$ of 5 km. Thus the model is considered to be stable with variations in space increments. The same sensitivity tests were performed for Section B of the San Andreas fault and similar results were observed.

7. SUMMARY AND CONCLUSIONS

A homogeneous time and space dependent stochastic model is developed to determine the likelihood of earthquakes along faults. Inclusion of temporal dependence is particularly important when modeling large magnitude earthquakes. Spatial dependence is found to be important when there is a variation in the frequency and size of earthquake activity along the same fault. The influence of one fault on another nearby parallel or crossing fault was not investigated because of the lack of substantiating evidence for their dependencies. In cases when several faults can be linked to the same tectonic mechanism, difficulties with quantifying the dependencies among faults prevented their study and application to the model.

The model is found to be relatively stable with variations in time and space increments. Selections of time and space increments were found to be dependent on the selection of the energy release scale and the corresponding state space vector. These increments, as well as the increments of energy release levels are also governed by the basic assumptions of the stochastic model for spatial and temporal dependence.

The comparison of the proposed model with the simple Poisson model reveals that lower probabilities for large magnitude events are obtained with the time and space dependent model when the fault is

characterized by very large events. Similarly, the current model represents the spatial influence of one section of a fault on an adjacent one, while the Poisson model assumes total spatial independence. It is therefore concluded that the time and space dependent model provides a more realistic representation of earthquake occurrences along faults where distinction can be made in the activity of various segments of that fault.

The stochastic earthquake occurrence model will be applied best in seismic hazard analyses of small geographical regions. It becomes computationally unfeasible when large areas with very long faults or major tectonic systems (such as the circum-Pacific belt) are considered. The model can be easily extended to determine the hazard at a specified site, provided the necessary attenuation relationship is available. In such applications of site hazard evaluations, it may be desirable to use a combination of the Poisson model for faults with relatively uniform activity together with the time and space dependent model. It is felt that the developments in this report represent a significant contribution towards the understanding and modeling of the earthquake phenomena for engineering seismic hazard analysis purposes.

8. REFERENCES

Benjamin, J. R. and Cornell, C. A. (1970), Probability, Statistics and Decision for Civil Engineers, McGraw-Hill Book Company, New York, New York.

Cotton, W. R., Hall, N. T. and Hay, E. A., (1979), "Holocene Behavior of the San Andreas Fault - San Juan Bautista to Point Arena, California," A Semi-Annual Technical Report for USGS, Grant No. 14-08-0001-18229.

Cornell, C. A. (1968), "Engineering Seismic Risk Analysis," Bulletin of the Seismological Society of America, Vol. 54, No. 5, pp. 1583-1606.

Der Kiureghian, A. and Ang, A. H-S. (October 1975), "A Line Source Model for Seismic Risk Analysis," Structural Research Series No. 419, University of Illinois at Urbana-Champaign, Urbana, Illinois.

Esteva, L. (1976), in Seismic Risk and Engineering Decisions, "Developments in Geotechnical Engineering 15," Elsevier Scientific Publishing, New York.

Hagiwara, Y. (March 1975), "A Stochastic Model of Earthquake Occurrence and the Accompanying Horizontal Land Deformations," Tectonophysics, Vol. 26, No. 1/2, pp. 91-101.

Hanks, T. C. and Kanamori, H. (1979), "A Moment Magnitude Scale," Journal of Geophysical Research, Vol. 84, No. B5, pp. 2348-2350.

Kiremidjian, A. S. and Shah, H. C. (November 1975), "Seismic Hazard Mapping of California," Report No. 21, John A. Blume Earthquake Engineering Center, Dept. of Civil Engineering, Stanford University, Stanford, CA.

Knopoff, L. and Kagan, V. (December 1977), "Analysis of the Theory of Extremes as Applied to Earthquake Problems," Journal of Geophysical Research, Vol. 82, No. 36.

Nur, A. (1978), "Nonuniform Friction as a Physical Basis for Earthquake Mechanics," Pageoph, Vol. 116, pp. 964-991.

Patwardhan, A. S., Kulkarni, R. B. and Tocher, D. (1980), "A Semi-Markov Model for Characterizing Recurrence of Great Earthquakes," Bulletin of the Seismological Society of America, Vol. 70, No. 1, pp. 325-347.

Perkaru, G. and Berckhemer, H. (1978), "A Magnitude Scale for Very Large Earthquakes," Tectonophysics, 49, pp. 189-198.

Rikitaki, T. (March 1975), "Statistics of Ultimate Strain of the Earth's Crust and Probability of Earthquake Occurrence," Tectonophysics, Vol. 26, No. 1/2, pp. 1-21.

Savage, J. C. and Burford, R. O. (1973), "Geodetic Determination of Relative Plate Motion in Central California," Journal of Geophysical Research, Vol. 78, No. 27, pp. 832-845.

Scholz, C. H. and Fitch, T. J. (1969), "Strain Accumulation Along the San Andreas Fault," Journal of Geophysical Research, Vol. 74, No. 27, pp. 6649-6666.

Shah, H. C., Mortgat, C. P., Kiremidjian, A. S. and Zsutty, T. C. (January 1975), "A Study of Seismic Risk for Nicaragua," Part I and II, The J. A. Blume Earthquake Engineering Center, Report Nos. 11 and 12, Dept. of Civil Engineering, Stanford University, Stanford, CA.

Shlien, S. and Toksoz, M. (1970), "A Clustering Model for Earthquake Occurrences," Bulletin of the Seismological Society of America, Vol. 60, No. 6, pp. 1765-1787.

Slemmons, D. B. (February 8, 1978), "Seismological Environment," a lecture at the EERI Seminar on Seismic Risk Analysis, Los Angeles, California.

Steinbrugge, K. V. (1960), "Creep on the San Andreas Fault," Bulletin of the Seismological Society of America, Vol. 50, No. 3, pp. 389-415.

Thatcher, W. (1975a), "Strain Accumulation and Release Mechanism of the 1906 San Francisco Earthquake," Journal of Geophysical Research, Vol. 80, No. 35, pp. 4862-4872.

Thatcher, W. (1975b), "Strain Accumulation on the Northern San Andreas Fault Zone Since 1906," Journal of Geophysical Research, Vol. 80, No. 35, pp. 4873-4880.

Thatcher, W. and Hanks, T. C. (1973), "Source Parameters of Southern California Earthquakes," Journal of Geophysical Research, 78, pp. 8547-8576.

Veneziano, D. and Cornell, C. A. (May 1974), "Earthquake Models with Spacial and Temporal Memory for Engineering Seismic Risk Analysis," R74-18, Structures Pub. No. 385, Dept. of Civil Engineering, Massachusetts Institute of Technology, Cambridge, Massachusetts.

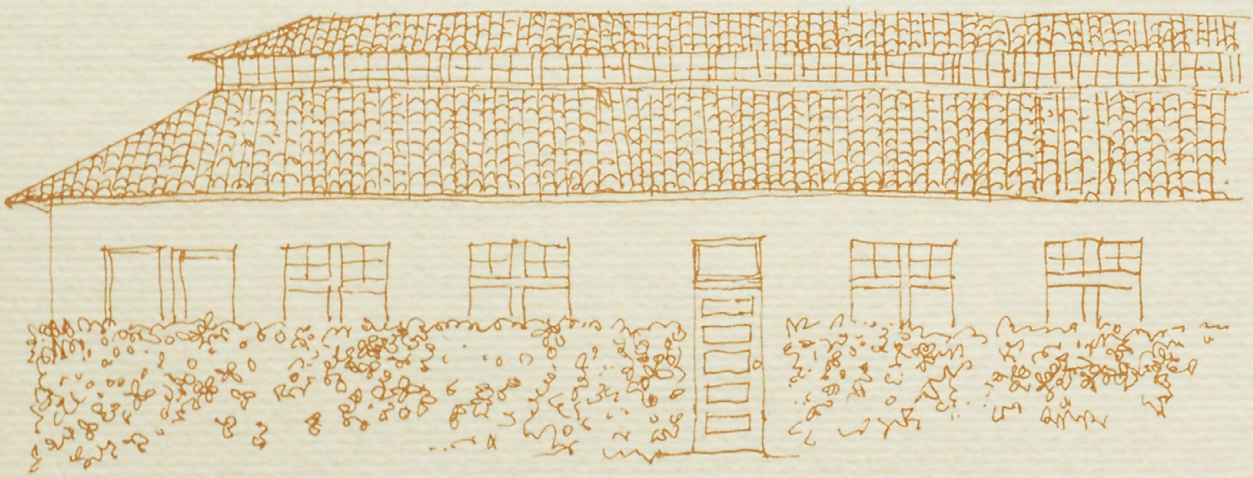

The John A. Blume Earthquake Engineering Center – Stanford University